Fully and partially iodinated germanane as a platform for the observation of the quantum spin Hall effect

J. E. Padilha,[1,*] L. B. Abdalla,[2] A. J. R. da Silva,[3,4] and A. Fazzio[3,5,†]

[1]*Universidade Federal do Paraná, Campus Avanado Jandaia do Sul, CP 49, 86900-000 Jandaia do Sul, PR, Brazil*

[2]*University of Colorado, Boulder, Colorado 80309, USA*

[3]*Instituto de Física, Universidade de São Paulo, CP 66318, 05315-970 São Paulo, SP, Brazil*

[4]*Laboratório Nacional de Luz Síncrotron, CP 6192, 13083-970 Campinas, SP, Brazil*

[5]*Centro de Ciências Naturais e Humanas, Universidade Federal do ABC, Santo André, 09210-170 São Paulo, Brazil*

(Received 2 September 2015; revised manuscript received 12 January 2016; published 27 January 2016)

Motivated by the recent isolation of the trivial insulator germanane, a fully hydrogenated germanene, we show that partially substituting hydrogen atoms with iodine on only one side of the material creates a two-dimensional topological insulator with a large band gap of 0.49 eV. This functionalization opens up different routes for the observation of the quantum spin Hall effect in fully two-dimensional materials. We also show that by creating nanoroads with the pattern functionalization of germanane by iodine in an ordered or disordered way, topologically protected interfaces states arise at the boundary of germanane/iodinated germanane.

DOI: 10.1103/PhysRevB.93.045135

I. INTRODUCTION

The quantum spin Hall effect (QSHE), proposed in 2005 by Kane and Mele for graphene [1] and by Zhang *et al.* in 2006 for HgTe/CdTe [2], has become a very exciting area of condensed matter physics. Its exquisite properties could change the paradigm of nanoelectronics. The electric current predicted by this effect may flow without dissipation. In addition to the potential applications in technology, it has boosted a whole new area of research in condensed matter physics, called topological insulators [3–5]. In the materials which the QSHE was initially designed, it was only verified experimentally in the heterostructure of HgTe/CdTe [6]. In graphene, due to the small spin-orbit coupling gap (SOC), its experimental verification becomes impractical [7,8]. Also, in the heterostructure of HgTe/CdTe, experimental observations are only possible at very controlled and low temperatures, since the SOC gap of this system is only 5 meV [6].

Several materials have been proposed to overcome the issue of the small SOC band gap, such as the elemental materials germanene (with a SOC gap of 29 meV) [9] and stanene (with a SOC gap of 100 meV) [10], and other binary compounds with band gaps that go from several meV to a few eV [11,12]. Besides the pristine materials, it was also reported that a functionalization with halogens in those structures could enhance the SOC gap [10,13–15], such as stanene and germanene with iodine, presenting a SOC gap of 0.34 and 0.30 eV, making those materials good candidates not only for the observation of the QSHE at room temperature, but for real applications in electronic devices. From the experimental point of view, only germanene was recently synthesized, and since it is strongly attached to a metal surface, its use in nanoelectronics is still limited [16]. Also, another important material, which was synthesized in 2013, is the germanane structure (Ge-H) [17], a fully hydrogenated germanene. This material is a trivial insulator with an electronic band gap of $\approx$1.46 eV, which could be used as a key ingredient for the construction of devices for the observation of the QSHE.

Motivated by the experimental realization of the trivial insulator germanane (Ge-H) [17], Seixas *et al.* [18] proposed a way to observe the QSHE in germanene by removing the hydrogen atoms in a pattern fashion, creating a germanene nanoroad inside germanane. By doing this, the topological insulator germanene is in contact with the trivial insulator germanane, and topologically protected edge states appear at the interface of the nanoroad. Those interface states are similar to the ones presented by germanene nanoribbons [19]. In this kind of situation, where the germanene structure is completely exposed from germanane, some issues could be present in its possible experimental realization: (1) The hydrogen atoms could be removed only on one side of the road, giving rise to magnetism [20], degrading the topological properties of the material; (2) as the region where the hydrogen atoms were removed became very reactive, the possible adsorption of other atoms could degrade the topological properties of the system; and (3) the SOC of germanene is also small (29 meV), so that in higher temperatures the QSHE will not be observed.

In this paper we show that the substitution of all hydrogen atoms with iodine on only one side of germanane creates a two-dimensional (2D) topological insulator with a large band gap of 0.49 eV. This functionalization opens up different routes for the observation of the quantum spin Hall effect in fully two-dimensional materials. We also show that by creating nanoribbons with this partially iodinated germanane, as well as by creating nanoroads with the pattern functionalization of germanene with iodine (partially or fully ordered or disordered), topologically protected interfaces states arise at the boundary of germanane/iodinated germanane.

II. MODELS AND METHODS

Our simulations were based on density functional theory (DFT) [21,22] as implemented in the OPENMX code [23,24]. For the exchange-correlation functional we used the generalized gradient approximation of Perdew, Burke, and

*jose.padilha@ufpr.br

†fazzio@if.usp.br

 ©2016 American Physical Society

Ernzerhof (GGA-PBE) [25]. The spin-orbit interaction was included via a norm-conserving, fully relativistic, j-dependent pseudopotential scheme [26]. Both the lattice constants as well as the atomic positions were relaxed until the residual forces were smaller than 0.001 eV/Å.

A QSH material in 2D is represented by a topological invariant $Z_2 = 1$, which is customarily referred to as ν_0 in 3D. To calculate the Z_2 invariant of the system we used the scheme proposed by Fu and Kane [5,27] as implemented by Abdalla *et al.* in Ref. [28]. The topological invariant Z_2 is calculated using the equation

$$(-1)^{Z_2} = \prod_{\text{TRIM}} \delta_{\Lambda_i}, \quad \delta_{\Lambda_i} = \frac{\text{Pf}[\omega(\Lambda_i)]}{\sqrt{\det \omega(\Lambda_i)}}, \tag{1}$$

where $\text{Pf}[\omega(\Lambda_i)]$ is the Pfaffian, Λ_i are the time reversal invariant momenta points (TRIMs), and $\omega_{nm}(\Lambda_i)$ is a unitary matrix that in a plane wave basis set code is given by

$$\omega_{nm} = \sum_{\vec{K}_j} -C^{\uparrow *}_{n,\Lambda_i,-2\Lambda_i-\vec{K}_j} C^{\downarrow *}_{m,\Lambda_i,\vec{K}_j} + \sum_{\vec{K}_j} C^{\downarrow *}_{n,\Lambda_i,-2\Lambda_i-\vec{K}_j} C^{\uparrow *}_{m,\Lambda_i,\vec{K}_j}, \tag{2}$$

where $C^{\sigma}_{n,\Lambda_i,\vec{K}_j}$ are the wave function coefficients. More details about this implementation may be found in Ref. [28].

We also calculated the Z_2 invariant using the method proposed by Soluyanov and Vanderbilt [29,30] for systems without inversion symmetry. This method tracks the evolution of the Wannier center of charges (WCCs) for an effective 1D system with fixed k_y in the subspace of occupied bands. The Wannier function (WF), related to a lattice vector R, is described as

$$|R,n\rangle = \frac{i}{2\pi} \int_{-\pi}^{\pi} dk e^{ik(R-x)} |u_{nk}\rangle. \tag{3}$$

The WF depends on a gauge choice for the Bloch states $|u_{nk}\rangle$. Following Marzari and Vanderbilt's description [31], to optimally localize the WF, we define WCCs as the mean value of the position operator $\bar{x} = \langle 0n|\hat{X}|0n\rangle$. In the limit of an infinite lattice, $\hat{X} \to i\frac{\partial}{\partial k_x}$, and Z_2 can be written as

$$Z_2 = \left[\sum_{\alpha} \bar{x}^{\text{I}}_{\alpha}(\text{TRIM}_1) - \bar{x}^{\text{II}}_{\alpha}(\text{TRIM}_1)\right] - \left[\sum_{\alpha} \bar{x}^{\text{I}}_{\alpha}(\text{TRIM}_2) - \bar{x}^{\text{II}}_{\alpha}(\text{TRIM}_2)\right], \tag{4}$$

where α is a band index of the occupied states and I and II are the Kramer partners. This equation tells us that an odd number of switchings between WCCs would make the Z_2 number odd, unveiling its topological nature. The topology of the system, the SOC band gap, and the band inversion picture were also verified by means of the hybrid functional of Heyd, Scuseria, and Ernzerhof (HSE06) [32,33] as implemented in the VASP code [34,35].

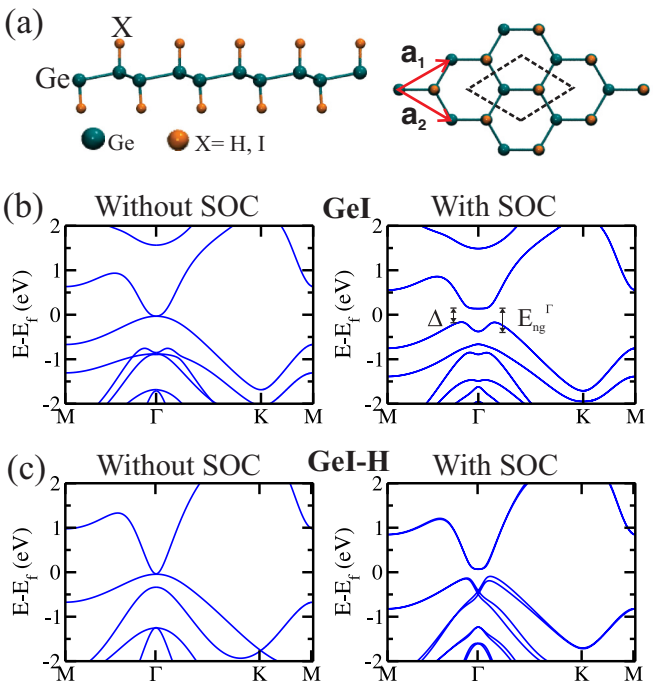

FIG. 1. (a) Schematic structure of the functionalized germanene Ge-X, where X represents the single functionalization by H and I or the binary compounds I-H. Band structure for (b) Ge-I and (c) Ge-I-H, without (with) spin-orbit coupling on the left (right) panel. E^{Γ}_{ng} and Δ represents the nontrivial gap opened at Γ by the SOC and the indirect band gap in the system.

III. RESULTS AND DISCUSSIONS

Initially, we studied a system composed of germanene functionalized on both sides by iodine [13–15] as well as germanene with hydrogen on one side and iodine on the other. The former was used to improve the SOC band gap in germanene and the last also to improve the SOC gap as to prevent the magnetism presented by half-hydrogenated germanene. As depicted in Fig. 1(a), we show a schematic representation of the systems considered in our simulations. The functional group (orange atoms) could be H and I. The germanane (fully hydrogenated germanene) is a semiconductor with a direct band gap of 1.54 eV [17]. When both hydrogen atoms are replaced with iodine, the system after relaxation increases its lattice constant from 4.06 Å for GeH to 4.32 Å for GeI. Without SOC the iodinated germanene is a zero gap semiconductor, where the valence and conduction bands touch each other only at the Γ point, and when the SOC is included, there is an opening of a nontrivial band gap of 0.51 eV at the Γ point, as depicted in Fig. 1(b). In addition, when only one hydrogen atom is replaced with an iodine, the behavior of the structural properties is quite similar to one with two iodine atoms. The lattice constant of the system is slightly small, around 4.22 Å, and the nontrivial band gap is around 0.48 eV, as depicted in Fig. 1(c). For both systems we obtained $Z_2 = 1$ by the Pfaffian method. In addition to the Pfaffian method, we present in Fig. 2 the evolution of the WCCs for germanane (GeH) [Fig. 2(a)], fully iodinated germanene (GeI) [Fig. 2(b)], and half-iodinated germanane (GeI-H) [Fig. 2(c)]. Corroborating with our results,

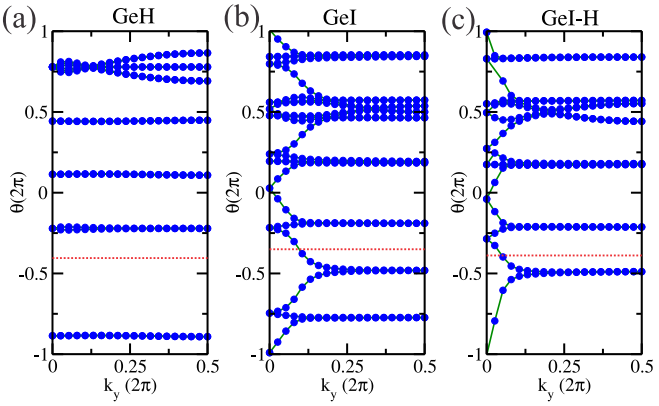

FIG. 2. Evolution of the Wannier charge centers (WCCs) between two TRIM points in the reciprocal plane $k_z = 0$ for (a) GeH, (b) GeI, and (c) GeI-H. In dashed red we have a reference line to track the number of Wannier center pairs switching in half of the Brillouin zone.

we can see that GeH is a trivial insulator and both GeI and GeI-H are $Z_2 = 1$ topological insulators.

In addition to the Z_2 invariant, one of the key characteristics presented by a 2D topological insulator is the presence of topologically protected edge/interface states when the material is contacted to a trivial insulator. Those topological states are presented in an odd number of Dirac cones. The limiting case for the observation of topologically protected edge states in a 2D topological insulator is by contacting this material with the vacuum and creating a nanoribbon. In Fig. 3 we show the band structure and local charge density around the Fermi level, for the zigzag and armchair nanoribbons of Ge-I and Ge-I-H. In this situation all hydrogen atoms in one or both sides are replaced by iodine. For the fully iodinated case, presented in Figs. 3(a) and 3(b), to avoid any interaction between the edges, we used a ribbon size of 7.7 nm for the armchair and 6.1 nm for the zigzag. We can clearly see the presence of the topological edge states (red lines) in the band structure, where both systems present a Dirac cone at the Γ point. Also, in Figs. 3(a) and 3(b) we present in the right panel a local charge density calculated around the Fermi level, showing that the Dirac cone is localized on the edges of the material. The same behavior is observed for the half-iodinated armchair and zigzag nanoribbons presented in Figs. 3(c) and 3(d). The behaviors of the armchair nanoribbons in both systems (G-I and Ge-I-H) are the same, with the edge states being completely degenerate. For the zigzag one in the half-iodinated case, there is a symmetry break due to relaxation effects, lifting the degeneracy between the edges.

Going beyond the discussion about the edge states that arises due to the bulk boundary correspondence when a topological insulator is connected to a trivial insulator, we can connect the ribbons considered in the previous results to the semiconducting germanane, creating what we call a nanoroad inside germanane (GeH). It is worth mentioning that this kind of technique to create such nanoroads is also used in graphene/graphane and graphene/fluorographene systems [36–38]. As depicted in Fig. 4, we present the results for the nanoroad created inside germanene by iodination of a single side [Fig. 4(a)] or both sides [Fig. 4(b)]. We show only the

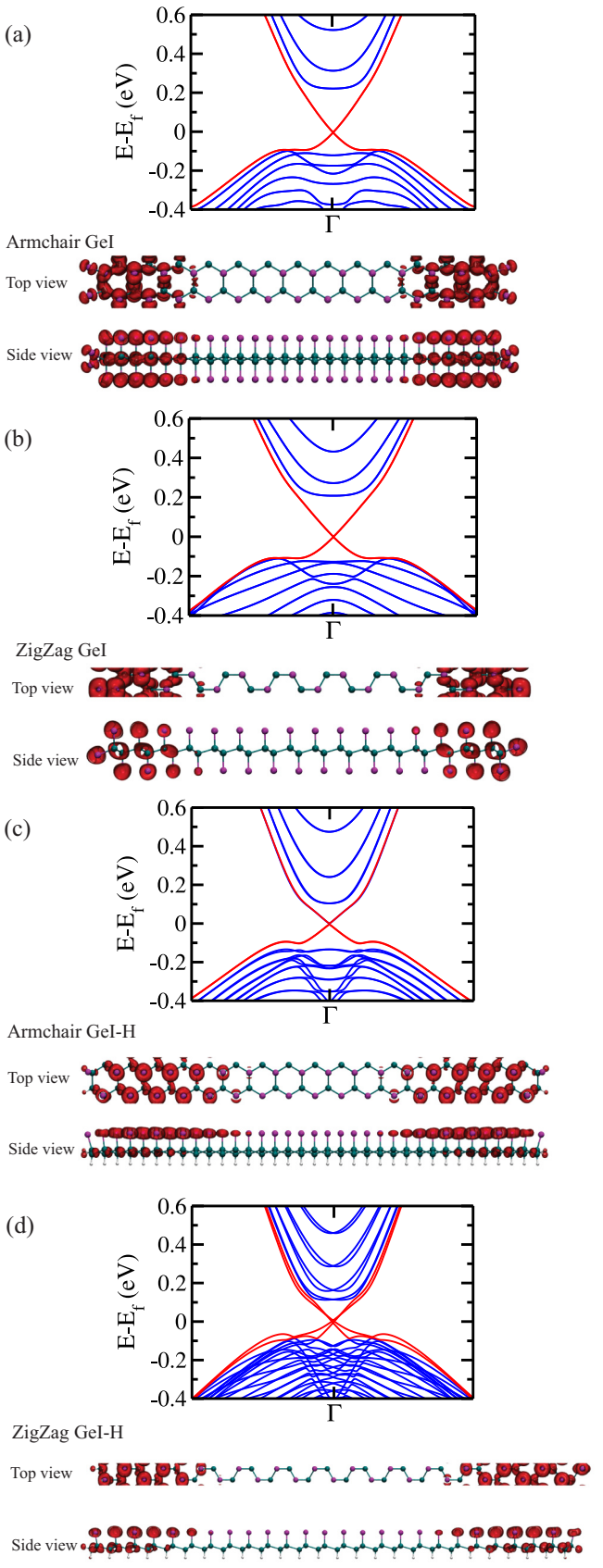

FIG. 3. Band structure (left) and local charge density integrated around 0.1 eV of the Fermi level (right) for an (a) armchair and (b) zigzag Ge-I nanoribbon and an (c) zrmchair and (d) zigzag Ge-I-H nanoribbon.

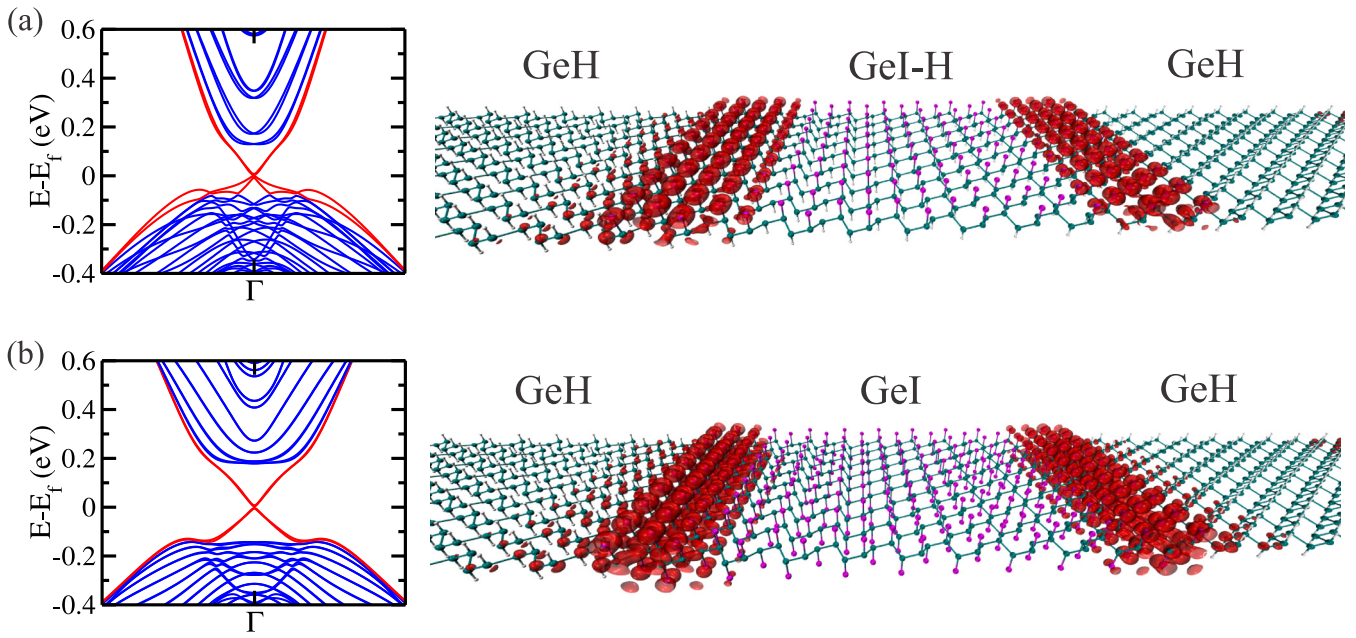

FIG. 4. Band structure for a zigzag nanoroad (left) and local charge density integrated around 0.1 eV of the Fermi level (right) for (a) Ge-I-H and (b) Ge-I.

results for the zigzag system, as the armchair one gives results similar to the ones previously shown for the nanoribbons. On the left panel we show the band structure and on the right the local charge density integrated around 0.1 eV, the Fermi level. As we can see, topologically protected Dirac cone states arise at the interface of the materials, being spatially localized in the vicinity of the interface of the functionalized material with the germanane. It is important to note that for the partially/fully iodinated nanoribbon/nanoroad, independently of the shape of the edge/interface (zigzag or armchair), the topological interface states will be always present.

Finally, in Fig. 5 we present a way to construct a device for the observation of the quantum spin Hall effect. In Fig. 5(a) (top) we schematically present the removal of the hydrogen atoms on only one or both sides of the trivial insulator germanane. This could be done in the same way that is done in graphene systems [36–38], as we have previously mentioned, by removing the hydrogen atoms in a desired pattern by, for example, hydrogen dissociation via plasma etching [39–41]. For example, one can create a single hydrogen vacancy or a double hydrogen vacancy that possess formation energies around 1.0 and 0.6 eV [18] and subsequently deposit the

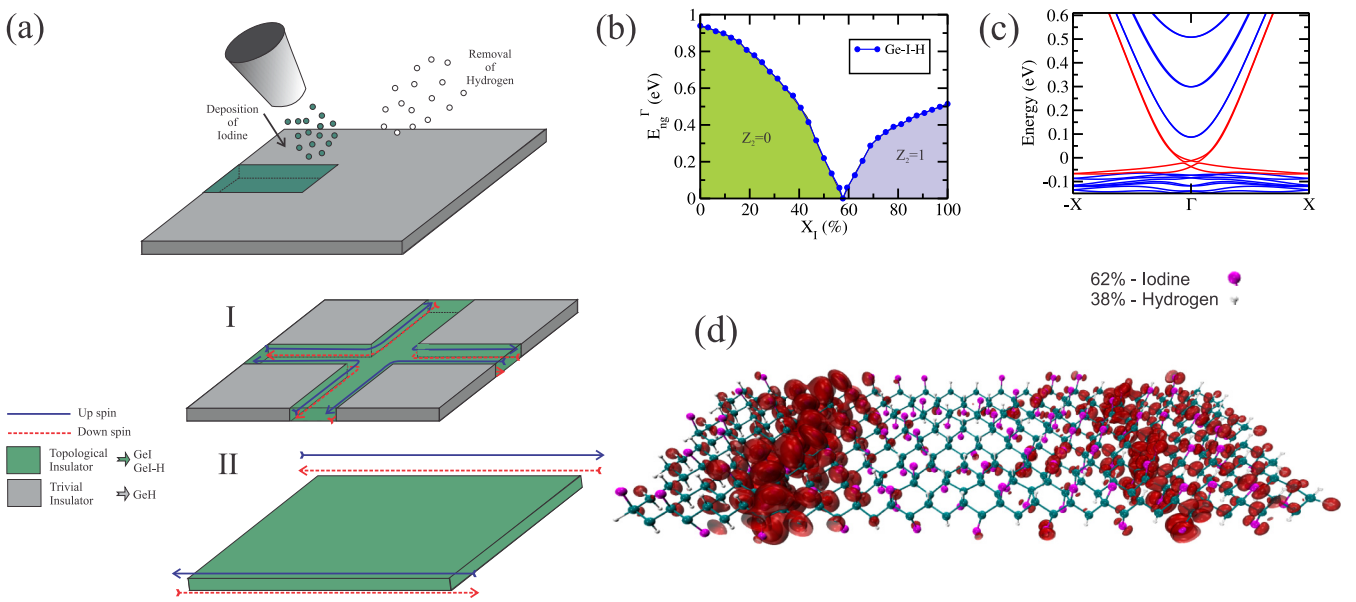

FIG. 5. (a) Schematic representation of possible configurations for the observation of the quantum spin Hall effect. (b) Evolution of the band gap at the Γ point as a function of the concentration of iodine in germanane. (c) Band structure of a nanoribbon with 62% of iodine. (d) Local density of states around the Fermi level for the ribbon considered in (c).

iodine in the vacant sites. For example, in our 7×7 supercell, the calculated formation energy of four hydrogen vacancies is ≈1 eV/hydrogen, and when the iodine atoms saturate the hydrogen vacant sites, it lowers the energy of the system by 0.89 eV/iodine, presenting that the energy cost to introduce iodine in the system is low. This kind of lithography could be used to construct patterns such as the one presented in Figs. 5(a) I–II by removing the atoms on one or both sites of the germanane layer. The first one represents the creation of the iodinated nanoroads inside germanane and the last one is the nanoribbon. In both situations, topologically protected edge states will arise at the edge/interface of the 2D topological insulator with the trivial one. However, it may occur that not all hydrogen atoms are removed from the system to create the nanoribbons or the nanoroads. Thus, it is important to understand if the presence of some reminiscent hydrogen atoms in the system will maintain the topologically protected edge states.

To describe the above situation and as the iodine atom will be randomly distributed, replacing the hydrogen atoms, we employed the special quasirandom structure (SQS) model proposed by Wei *et al.* [42] to construct the geometries. This method provides a simple way to determine, via first-principles calculations, the structural and electronic properties of a random distribution of atoms with a supercell approach. Supercells with 98 atoms of Ge were used (7×7 supercell), and the iodine concentrations (replacing the hydrogen) were varied from 0% (trivial insulator) to 100% (2D topological insulator). Depicted in Fig. 5(b) is the band gap at the Γ point as a function of iodine concentration. From the adiabatic continuity argument, as the band gap closes going from a trivial insulator (0% iodine) to a topological insulator (100% iodine), we conclude that there is a topological phase transition around 58%, so that for all concentrations larger than 58%, the material is a 2D topological insulator. To verify this assumption, we present in Fig. 5(c) the band structure of a nanoribbon with an iodine concentration of 62%, and as we can see, there are topologically protected edge states in its electronic structure. The local density of states around the Fermi level for the edge states is presented in Fig. 5(d). In this way, even with a random distribution of iodine/hydrogen atoms inside germanane, the topologically protected edge states will appear.

IV. CONCLUSIONS

In conclusion, we show that, with the substitution of hydrogen atoms with iodine on only one side of germanane, the system is a 2D topological insulator with a band gap of 0.49 eV. This functionalization opens up different routes for the observation of the quantum spin Hall effect in fully two-dimensional materials. We also show that by creating nanoroads or nanoribbons with the pattern functionalization of germanene with iodine in an ordered or disordered fashion, topologically protected interface states arise.

ACKNOWLEDGMENTS

This work was supported by the Brazilian agencies FAPESP, CNPq, and CAPES. We would like to acknowledge computing time provided on the Blue Gene/Q supercomputer supported by the Research Computing Support Group (Rice University) and Laboratório de Computação Científica Avançada (Universidade de São Paulo). We also acknowledge Dr. A. A. Soluyanov for sharing the code to calculate the WCCs with VASP.

[1] C. L. Kane and E. J. Mele, Phys. Rev. Lett. **95**, 226801 (2005).
[2] B. A. Bernevig, T. L. Hughes, and S.-C. Zhang, Science **314**, 1757 (2006).
[3] M. Z. Hasan and C. L. Kane, Rev. Mod. Phys. **82**, 3045 (2010).
[4] X.-L. Qi and S.-C. Zhang, Rev. Mod. Phys. **83**, 1057 (2011).
[5] Y. Ando, J. Phys. Soc. Jpn. **82**, 102001 (2013).
[6] M. König, S. Wiedmann, C. Brüne, A. Roth, H. Buhmann, L. W. Molenkamp, X.-L. Qi, and S.-C. Zhang, Science **318**, 766 (2007).
[7] H. Min, J. E. Hill, N. A. Sinitsyn, B. R. Sahu, L. Kleinman, and A. H. MacDonald, Phys. Rev. B **74**, 165310 (2006).
[8] Y. Yao, F. Ye, X.-L. Qi, S.-C. Zhang, and Z. Fang, Phys. Rev. B **75**, 041401 (2007).
[9] C. C. Liu, W. X. Feng, and Y. G. Yao, Phys. Rev. Lett. **107**, 076802 (2011).
[10] Y. Xu, B. Yan, H.-J. Zhang, J. Wang, G. Xu, P. Tang, W. Duan, and S.-C. Zhang, Phys. Rev. Lett. **111**, 136804 (2013).
[11] J. E. Padilha, L. Seixas, R. B. Pontes, A. J. R. da Silva, and A. Fazzio, Phys. Rev. B **88**, 201106 (2013).
[12] F.-C. Chuang, L.-Z. Yao, Z.-Q. Huang, Y.-T. Liu, C.-H. Hsu, T. Das, H. Lin, and A. Bansil, Nano Lett. **14**, 2505 (2014).
[13] C.-C. Liu, S. Guan, Z. Song, S. A. Yang, J. Yang, and Y. Yao, Phys. Rev. B **90**, 085431 (2014).
[14] Y. Ma, Y. Dai, C. Niua, and B. Huanga, J. Mater. Chem. **22**, 12587 (2012).
[15] C. Si, J. Liu, Y. Xu, J. Wu, B.-L. Gu, and W. Duan, Phys. Rev. B **89**, 115429 (2014).
[16] M. E. Dávila, L. Xian, S. Cahangirov, A. Rubio, and G. Le Lay, New J. Phys. **16**, 095002 (2014).
[17] E. Bianco, S. Butler, S. Jiang, O. D. Restrepo, W. Windl, and J. E. Goldberger, ACS Nano **7**, 4414 (2013).
[18] L. Seixas, J. E. Padilha, and A. Fazzio, Phys. Rev. B **89**, 195403 (2014).
[19] L. Matthes and F. Bechstedt, Phys. Rev. B **90**, 165431 (2014).
[20] X.-Q. Wang, H.-D. Li, and J.-T. Wang, Phys. Chem. Chem. Phys. **14**, 3031 (2012).
[21] P. Hohenberg and W. Kohn, Phys. Rev. **136**, B864 (1964).
[22] W. Kohn and L. J. Sham, Phys. Rev. **140**, A1133 (1965).
[23] The DFT code, OPENMX, is available at the web site http://www.openmx-square.org in the constitution of the GNU General Public Licence.
[24] T. Ozaki, Phys. Rev. B **67**, 155108 (2003).
[25] J. P. Perdew, K. Burke, and M. Ernzerhof, Phys. Rev. Lett. **77**, 3865 (1996).
[26] G. Theurich and N. A. Hill, Phys. Rev. B **64**, 073106 (2001).
[27] L. Fu and C. L. Kane, Phys. Rev. B **74**, 195312 (2006).

[28] L. B. Abdalla, J. E. Padilha, T. M. Schmidt, R. H. Miwa, and A. Fazzio, J. Phys.: Condens. Matter **27**, 255501 (2015).
[29] A. A. Soluyanov and D. Vanderbilt, Phys. Rev. B **83**, 035108 (2011).
[30] A. A. Soluyanov and D. Vanderbilt, Phys. Rev. B **83**, 235401 (2011).
[31] N. Marzari and D. Vanderbilt, Phys. Rev. B **56**, 12847 (1997).
[32] J. Heyd, G. E. Scuseria, and M. Ernzerhof, J. Chem. Phys. **118**, 8207 (2003).
[33] J. Heyd, G. E. Scuseria, and M. Ernzerhof, J. Chem. Phys. **124**, 219906 (2006).
[34] G. Kresse and J. Furthmüller, Phys. Rev. B **54**, 11169 (1996).
[35] G. Kresse and D. Joubert, Phys. Rev. B **59**, 1758 (1999).
[36] M. A. Ribas, A. K. Singh, P. B. Sorokin, and B. I. Yakobson, Nano Res. **4**, 143 (2011).
[37] A. K. Singh, and B. I. Yakobson, Nano Lett. **9**, 1540 (2009).
[38] J. M. Almeida, A. R. Rocha, A. K. Singh, A. Fazzio, and A. J. R. da Silva, Nanotechnology **24**, 495201 (2013).
[39] Y. Wang, X. Xu, J. Lu, M. Lin, Q. Bao, B. Özyilmaz, and K. P. Loh, ACS Nano **4**, 6146 (2010).
[40] C. D. Reddy, Q. H. Cheng, V. B. Shenoy, and Y. W. Zhang, J. Appl. Phys. **109**, 054314 (2011).
[41] M. Wojtaszek, N. Tombros, A. Caretta, P. H. M. van Loosdrecht, and B. J. van Wees, J. Appl. Phys. **110**, 063715 (2011).
[42] S.-H. Wei, L. G. Ferreira, J. E. Bernard, and A. Zunger, Phys. Rev. B **42**, 9622 (1990).